A Molecular Dynamics Study of Polyethylene Crystallization

T. A. Kavassalis* and P. R. Sundararajan*

Xerox Research Centre of Canada, 2660 Speakman Drive, Mississauga, Ontario, Canada L5K 2L1

Received December 2, 1992; Revised Manuscript Received April 26, 1993

ABSTRACT: Molecular dynamics simulations of model polyethylene chains of various lengths were performed. The occurrence of a few gauche states promotes long range attractive interactions between segments and causes the chain to fold into lamellae, via a global collapse mechanism. In the absence of the torsion potential, a two stage collapse process was seen, in which the chain forms local collapsed domains, which then coalesce into a large lamella. Simulations corresponding to elevated temperatures showed similar features. The calculated radii of gyration R_g of chains of various lengths show the same trend as the experimental results on solution crystallized polyethylene. The predominance of the trans conformation in the collapsed state indicates that substantial local order might be present in the melt.

Polymer crystallization has been the subject of several studies over the last 40 years.[1-6] One of the intriguing properties of polymers is their tendency not to form perfect crystals and in many cases to not form crystals at all. Those which do often exhibit varying degrees of crystallinity depending upon the conditions under which the material was formed, the treatment history, and of course, the chemical constitution. Many polymer technologies today attempt to exploit the role of material history on final product properties such as, for example, the use of high shear extrusion to tailor the processing properties of high density polyethylene.

Polymorphism is another characteristic of crystallizable polymers, which depends on the sample history. Even simple polymers such as polyethylene can exhibit a variety of crystalline morphologies. Apart from the possibility of more than one crystalline structure which could be due to different modes of packing of the chains or due to conformational variance,[7] the crystal habit formed during crystallization from solution or the melt depends on factors such as the degree of supercooling, concentration, etc.

Crystallization from solution or the melt results in a lamellar morphology. The arrangement of the molecular chains in the lamellae has been a topic of intense investigation and controversy. The simplest model is one in which the chains are folded in a regular manner, with the chain which leaves the lamellar surface reentering at the adjacent site (adjacent reentry model).[1,8,9] This model, however, was challenged by Flory[10,11] on kinetic and statistical mechanical considerations, and he favored a switchboard model in which the reentry is predominantly nonadjacent. On the basis of neutron scattering experiments from solution and the melt and calculations of the scattering intensities, Flory and Yoon[12,13] showed the nonadjacent reentry model to be consistent with the results of the scattering experiments. The scattering experiments of Sadler and Harris[14] on melt crystallized polyethylene led to the conclusion that up to about 40% of the folds could be adjacent. From Monte Carlo simulations, Mansfield[15] concluded that the combined adjacent and next-nearest-neighbor reentry never falls below 50%. The work of Hoffman[16] favors a predominantly adjacent reentry model.

In an attempt to gain some insight into the physical mechanism of polyethylene crystallization and in particular the role of the atomic level interactions, we have constructed and simulated several models of polyethylene at the molecular level, using molecular dynamics (MD) methods. The features of chain folding, the evolution of the lattice, and the influence of temperature which emerged from these simulations are described in this paper.

Molecular dynamics simulations of the polyethylene chain have been reported in the past by others. Roe and co-workers[17-22] performed such simulations using chains below, at, and above the glass transition temperature. They employed a system consisting of a cubic box containing up to 2000 CH_2 units (usually chains of up to 50 units in length). Zúñiga et al.[23] analyzed the transitions between rotational isomers in chains of 100 CH_2 units. de Pablo, Laso, and Suter[24] simulated chains of 60 CH_2 units below and above the melting temperature, using a continuum-configurational bias Monte Carlo method. Starting from an "extended chain" crystalline conformation, Noid et al.[25,26] performed simulations of the melting process and analyzed the change in the chain conformation with time and temperature. Generally, except for the results of Noid et al., the features of chain dynamics which we report in this paper were not observed in the work of the above authors.

Description of the Methodology

Various starting geometries were used for the simulations: (i) a single chain of polyethylene with 500, 750, 1000, or 2000 CH_2 units, with the skeletal bonds initially in the all-trans conformation; (ii) a single chain of 1000 CH_2 units, with the bonds in conformations corresponding to the rotational isomeric state distribution (for the generation of this chain, the tolerance of acceptance for the trans (t) (180°) and gauche ($g^{\pm}$) (±60°) rotation angles was set at 20°; the difference in energy between the t and $g^{\pm}$ states was taken to be 600 kcal·mol^{-1}); (iii) a set of four chains, each with 500 CH_2 units, initially in the all-trans conformation and placed in random orientation with respect to one another, but in close contact. Most of the discussion in this paper will be concerned with an isolated chain of 1000 units, with the all-trans starting conformation.

Each methylene unit was treated as a united atom, i.e., as a single sphere. This approximation of treating a nonspherical unit as a spherical entity would have its own consequences, but this was dictated by the effort to simplify the calculations. However, one simulation was performed with a chain of 500 CH_2 units, which included the hydrogens explicitly. The simulations were carried out using the Polygraf (version 3.0 and 3.1, Molecular Simulations Inc.) molecular modeling code. The time evolution of the chain conformations, up to 1000 ps, was simulated using the canonical (constant T) Nosé-Hoover

0024-9297/93/2226-4144$04.00/0

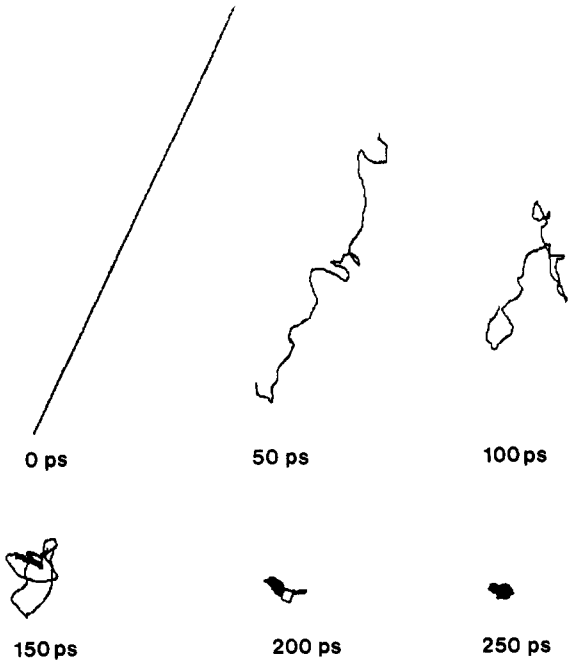

Figure 1. Time evolution of change in shape of a polyethylene chain with 1000 CH_2 units, at 300 K.

molecular dynamics method.[27] The constant T Nośe–Hoover method was chosen to be consistent with real phase transitions which occur at constant temperature and involve a heat exchange with the surroundings. Simulation temperatures of 300, 400, 500, and 600 K were employed. For systems with a united atom representation of the methylene group, an integration time step of 0.001 ps was used. The model system with explicit hydrogen atoms required a time step of 0.0002 ps. A relaxation constant of 0.10 ps for the heat bath variable was used throughout. The atomic force field used here is the Dreiding II potential,[28] which includes quadratic functions for bond length and bond angle deviations from their equilibrium values and a cosine term with a barrier height of 2 kcal·mol^{-1} for the torsional potential. Both short and long ranged nonbonded interactions were modeled by the Lennard–Jones 6–12 function, with a nonbonded cutoff distance of 10.5 Å. The equilibrium geometries and parameters for the force field are the same as those described by Mayo, Olafson, and Goddard.[28]

Results and Discussion

Collapse of the Chain Leading to Folding. Applying the MD prescription described above, the collapse of the model polyethylene chain, with 1000 units, is seen to follow the progression depicted in Figure 1. In the simulation that generated this sequence of conformations, the full molecular force field was included and the simulation temperature was set at 300 K. The system temperature fluctuations were always within 15 deg of the mean value. The sequence of snapshots shown in Figure 1 is not too unlike what one would expect for a fully extended elastic band that is suddenly relaxed. We will refer to this type of collapse process as a global collapse. By this term, we refer to the total simultaneous collapse of the entire structure. Later we will contrast this to a collapse process which proceeds via a two step mechanism: a local collapse, forming compact domains which subsequently coalesce to yield a fully collapsed state.

The initial, all-trans state (all torsion angles set to 180°) is shown in the upper left hand corner of Figure 1. The conformational transformations seen in Figure 1 indicate

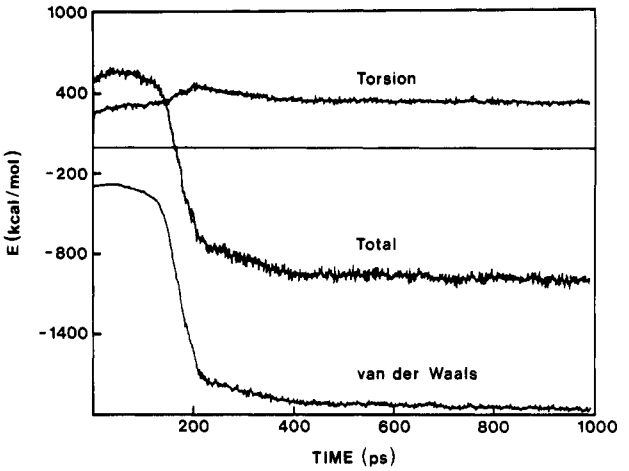

Figure 2. Variation of the torsional and van der Waals components of the energy and the total energy as a function of time.

that while this conformation is low in energy from the perspective of the short range steric interaction, it does not have a low nonbonded energy component. Any distortion of some of the skeletal bonds away from the all-trans conformation leads to a lower energy due to the nonbonded interaction between units separated by more than 5 Å, which is the typical short range diad interaction distance. The non-zero attractive force which extends over large distances is the driving force for the collapse process. The variation of the nonbonded, torsional, and total energies with time is shown in Figure 2. As the collapse process proceeds, the nonbonded and total energies decrease significantly (both by ~1.6 (kcal/mol)/bond) within the first 400 ps. The coupling of this system to the heat bath at 300 K using the Nosé–Hoover method leads to an overall drop in energy. The increase in the torsion energy from zero at the initial state to ~460 kcal/mol up to 200 ps for the entire structure is essentially due to the torsional barrier contribution as some of the bonds change to the gauche conformation and the deviation of the bonds changes from perfect staggering. The finite persistent torsion energy of ~0.35 (kcal/mol)/bond beyond 200 ps is essentially due to the presence of nonstaggered conformations (some of the torsion angles in the trans and gauche conformations deviate from perfect staggering by >20 deg). Figure 2 shows that in spite of the increase in the torsion energy during the first 200 ps, the nonbonded and total energies decrease during this time due to the precipitation of attractive interactions between the chain segments. The emergence of a few gauche conformations does not contribute significantly to the total energy since the nonbonded energy difference between the tt and tg$^{\pm}$ conformations is only ~500 cal/mol. Although we discuss here the results of one simulation, the run-to-run reproducibility of the results has been verified.

After 1000 ps of MD simulation a lamellar structure with "hexagonal symmetry" and close packing density has formed, as depicted in the two perspectives in Figure 3. The distance between the chains in the "ordered" array ranges from 4.2 to 5.2 Å, which is similar to the distance between the chains in the crystal structure of polyethylene. The all-trans structure is intrinsically unstable for the long chain, and the tendency to form a folded, lamellar structure predominates. The average number of methylene units in a run of all-trans segments is about 30 units, which corresponds to approximately 40–45 Å. A striking feature of this conformation is the roughly equal number of trans segments that display adjacent versus nonadjacent reentry of the chain into the lamella. The simulations

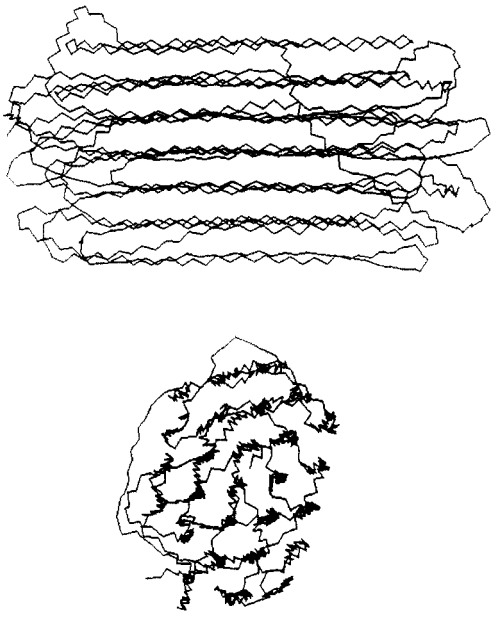

Figure 3. Two orthogonal perspectives of the lamellar structure formed with a polyethylene chain of 1000 CH_2 units, after 1000 ps at 300 K.

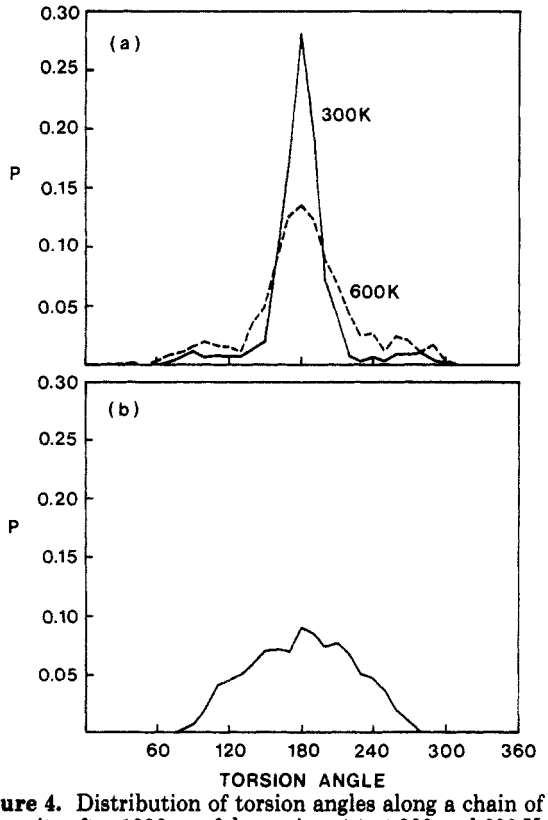

Figure 4. Distribution of torsion angles along a chain of 1000 CH_2 units after 1000 ps of dynamics: (a) at 300 and 600 K, with torsion energy; (b) 300 K, without torsion energy contribution.

with a chain of 500 CH_2 units with explicit hydrogens led to similar results.

The population density (P_i) of the torsion angles along the chain with 1000 CH_2 units, after 1000 ps at 300 K is shown in Figure 4a. The values of P_i were calculated simply as

$$P_i = n_i / \sum n_i \qquad (1)$$

where n_i is the number of bonds in a conformation with the dihedral angle i (i = 0–350°). It is seen that the conformation of the bonds, even after lamellar formation, is predominantly trans, with a significant occurrence of

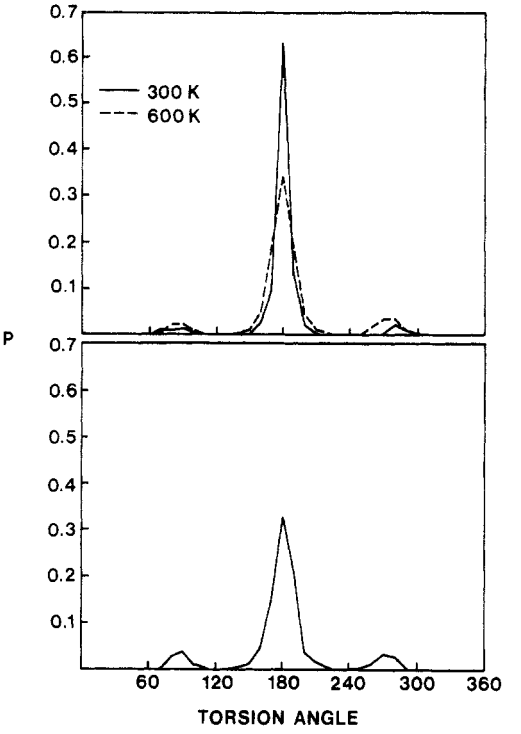

Figure 5. Distribution of torsion angles along a chain of 1000 CH_2 units after energy minimizing the snapshot after 1000 ps of dynamics: (a) at 300 and 600 K, with torsion energy; (b) 300 K, snapshot originally generated without the torsion energy contribution.

nonstaggered conformations (~30-deg deviation from 180° and a large departure from ±60°). The near-gauche population is very small. There is virtually no conformation corresponding to ±60°. The large deviation of the torsion angles from perfect staggering is a consequence of treating the CH_2 group as a spherical united atom. The torsion angle distribution upon energy minimization of the structure corresponding to 1000 ps is shown in Figure 5a. The distributions corresponding to the trans and gauche states become sharper, and the trans population shows a significant increase compared to that in Figure 4a. The energy minimization causes the states intermediate between trans and gauche to shift toward the former. Thus, the presence of a few near-gauche conformations with a large population of trans states seems to be sufficient for the chain folding to occur in a pattern, as seen in Figure 3.

The collapse process clearly proceeds via the global collapse mechanism in this case. During the course of the collapse, no evidence of any intermediate structures was seen and in particular there was no formation of locally collapsed domains. This was the case for structures with 500 and 750 methylene units as well. In the case of the "lower molecular weight" chains with 500 and 750 CH_2 units, the lamellar spacing varied between 25 and 35 Å, with both adjacent and nonadjacent reentry occurring with equal numbers of short and long straight chain segments. The lattice was not as well ordered as with the chain containing 1000 CH_2 units.

The above discussion applies to a polymer system in the vacuum state. In the melt, the collapse of the polymer will be complicated by intermolecular interactions and, in the solution, by the solvent influence as well. The influence of neighboring chains was indicated in the present study as follows: A simulation was performed with a cluster of four chains, each with 500 CH_2 units, the chains having been placed initially in arbitrary orientation with respect to one another. After about 700 ps, the lamellar spacing

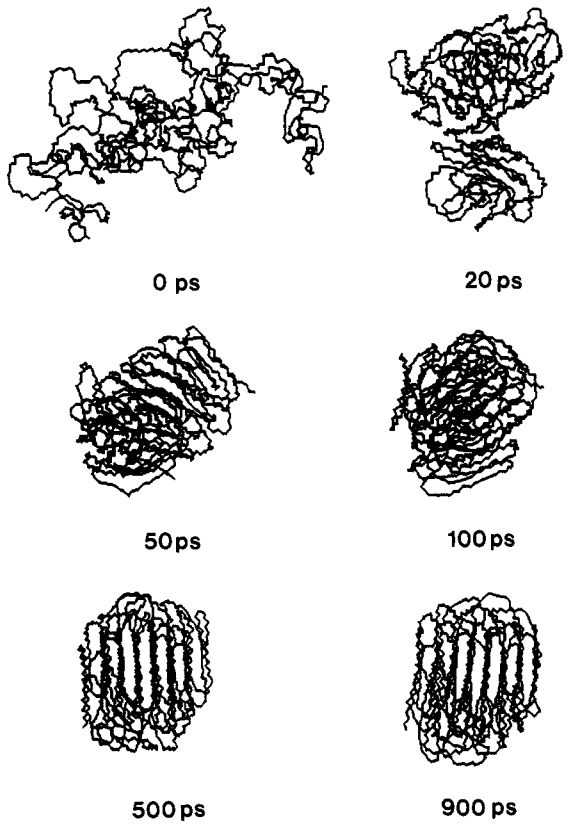

Figure 6. Time evolution of change in shape of a polyethylene chain with 1000 CH_2 units, at 300 K. The dihedral angle population of this chain at 0 ps corresponds to the rotational isomeric state distribution.

increased to ~50 Å in this case (as compared to 25–35 Å for the single chain cited above), confirming the effect of intermolecular interactions. This contrasts the results of Roe et al.[17-22] in which no such folding was observed with simulations with a cubic box containing multiple chains. However, the Monte Carlo simulations of de Pablo, Laso, and Suter[24] show hairpin configurations and the presence of long-lived kinks and bends due to the gauche population.

Chain with Initial Rotational Isomeric State (RIS) Distribution. Figure 6 shows the sequence of conformations of a polyethylene chain with 1000 CH_2 units and the initial RIS distribution of states, during the MD simulation at 300 K. Due to the initial presence of a large number of gauche conformations, the collapse of the chain proceeds with the vicinal sequences of trans bonds aggregating together to form local folded domains, which then coalesce to a lamellar morphology as for the 500- or 900-ps snapshot shown in this figure. An enlarged view of the lamellar structure is shown in Figure 7. The hexagonal packing of the chain is evident, and both adjacent and nonadjacent types of folds occur. It is interesting to note that the chain with an initial RIS distribution of states also formed lamellar folded chain morphology similar to the chain with an initial all-trans structure. The dimension of the lamella is 40-50 Å, which is also similar to that calculated for the morphology shown in Figure 3 above.

The distributions of torsion angles for the initial conformation and for the 600-ps snapshot are shown in Figure 8. It is seen that although initially the gauche states are of significant occurrence, the trans state population increases profusely during the collapse of the chain in the MD simulation. The population density of the trans and gauche states for the 600-ps structure in this figure do not differ appreciably from that shown in Figure 4a for the collapsed structure with the initial all-trans conformation.

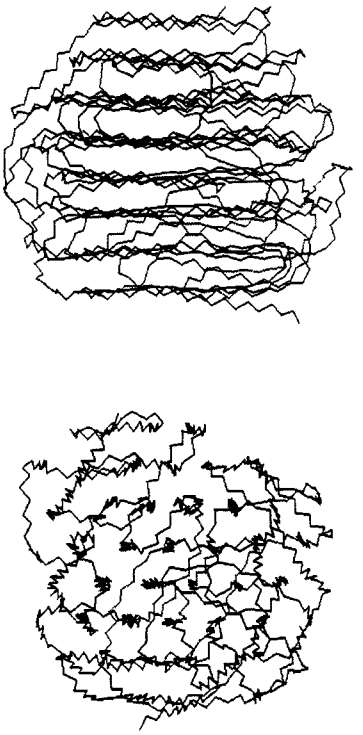

Figure 7. Two orthogonal perspectives of the lamellar structure formed with a polyethylene chain of 1000 CH_2 units, initially with RIS distribution of dihedral angles, after 600 ps at 300 K.

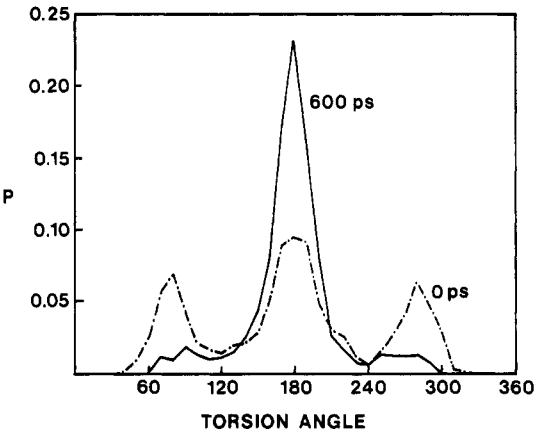

Figure 8. Distribution of torsion angles along a chain of 1000 CH_2 units: (- - -) initial RIS distribution (—) after 600 ps at 300 K.

Radius of Gyration. A plot of R_g as a function of the time of the simulation is shown in Figure 9a. It is seen that, consistent with the collapse of the chain, R_g decreases dramatically within the first 200 ps and reaches an asymptotic value. This result is similar to that of Noid et al.[25] which shows a significant reduction in R_g in the first few picoseconds of dynamics. Figure 9b shows the variation of R_g for the chain with 1000 CH_2 units, for four different temperatures. It is interesting to note a hump in the curve corresponding to about 150 ps in both Figure 9a,b, it being pronounced in the curve corresponding to the simulation at 600 K. This is traced to the contraction followed by an expansion of the chain during the dynamics between 80 and 150 ps and a collapse again. Initially, up to about 150 ps, with locally collapsed domains, the chain tends to be compact. However, at 150 ps, a significant expansion is seen, which increases the R_g. The chain then collapses back with a consequent decrease in R_g. Note that this occurs not only with the simulation at 600 K but also in all the cases shown in Figure 9 to a lesser extent. The factors which dictate this behavior are not understood

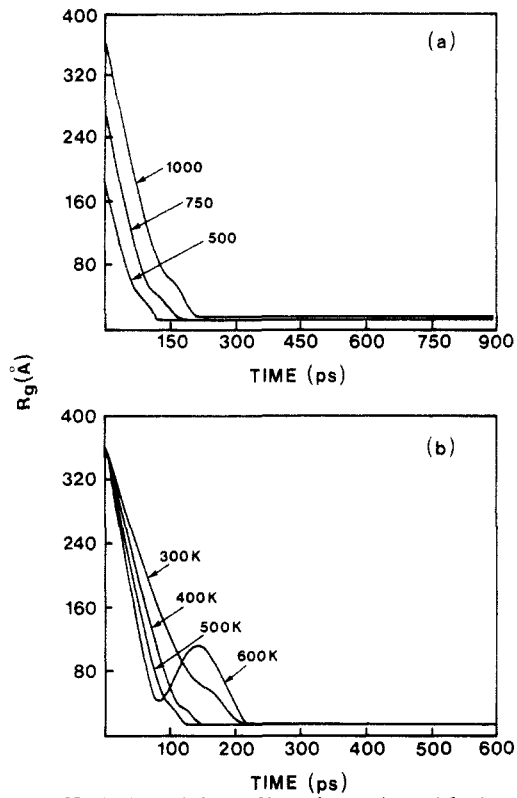

Figure 9. Variation of the radius of gyration with time for (a) chains with 500, 750, and 1000 CH_2 units and (b) the chain with 1000 CH_2 units, at 300, 400, 500, and 600 K.

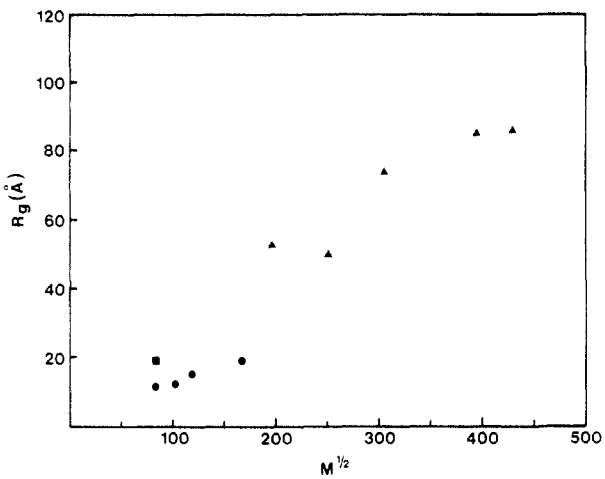

Figure 10. Variation of the "converged" values of R_g with $M^{1/2}$ is shown: (●) this work, with isolated chains; (■) simulation with 4 chains of 500 CH_2 units each; (▲) experimental results taken from Sadler and Keller.[29,30]

at this time but will be pursued in future work.

The results of Sadler and Keller[29,30] reported that the measured radius of gyration, R_g, was unaffected by molecular weight during crystallization from the melt, and a smaller R_g was noted for crystallization from solution. Figure 10 shows a plot of R_g as a function of $M^{1/2}$, for the simulated structures with 500, 750, and 1000 CH_2 units respectively, after more than 700 ps. Note that only one conformation was used to compute these values, which are therefore not ensemble averages. Also shown in this figure are the results taken from Table I of refs 29 and 30 on the R_g of solution grown single crystals. Sadler and Keller noted the insensitivity of R_g to molecular weight in this case. If the experimental results are linearly extrapolated to lower molecular weights, the calculated values of R_g from the simulation studies fall below those of the

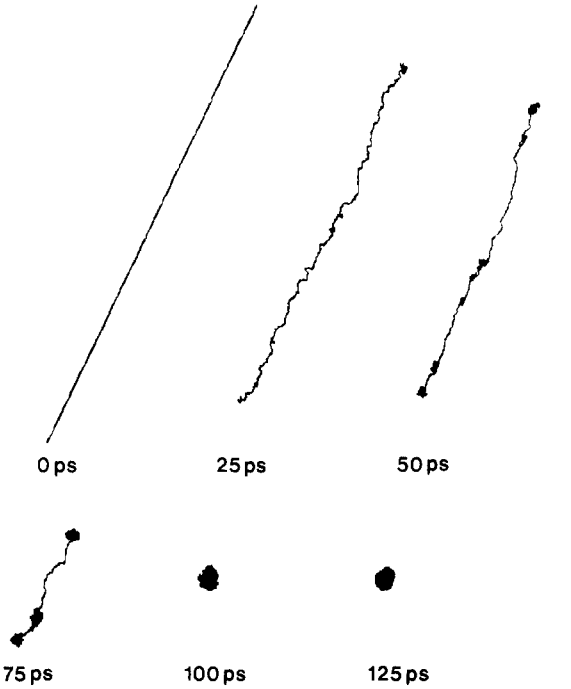

Figure 11. Time evolution of change in shape of a polyethylene chain with 1000 CH_2 units, corresponding to the simulation with no torsional potential.

real system of solution grown crystals. This is not surprising, however, since we are dealing with isolated chains here. The influence of multiple chains and hence the presence of intermolecular interactions, is seen in the results shown in Figure 10. Here the R_g was calculated from a simulation containing four chains, each with 500 CH_2 units, initially randomly placed with respect to one another. The collapse process included intertwining of the chains and lamellar type folding. The R_g, in this case, nearly doubles as compared to that of a single chain. Thus, the effect of multiple chains is to increase the lamellar dimension and the R_g. This agrees with the experimental observation that the measured R_g in the case of melt crystallized polyethylene is significantly higher than that for solution crystallization. The number of chains participating in the intermolecular interaction in the melt can be expected to be significantly higher than in the case of dilute solution crystallization. In any case, the trend in the variation of R_g with $M^{1/2}$, as seen from solution crystallization, is well reproduced by the present simulation. In addition, between 300 and 400 K, the calculated temperature coefficient of R_g is -0.9×10^{-3} K^{-1}, which is similar to the experimental value[31] of $d \ln \langle r^2 \rangle_0 / dT \approx -1 \times 10^{-3}$ K^{-1} (the latter corresponds to experimental measurements in the range 390–450 K). It is interesting to note that this reasonable agreement was achieved using an isolated chain for the simulations and that the present result is close to the value of -1.1×10^{-3} K^{-1} reported by dePablo, Laso, and Suter[24] based on simulations with intermolecular constraints imposed by the other chains in the periodic box.

Role of the Torsional Potential. In an effort to understand the role of the torsional potential on the collapse process and the final folded chain morphology, a series of molecular dynamics simulations were performed with polyethylene chains without the torsional potential. Figure 11 depicts the sequence of conformations that led to the collapsed state over the first 125 ps of a 1000-ps simulation. There is a very distinct difference between the conformations in this figure and those seen in Figure 1. Figure 11 displays an intermediate state with locally

collapsed domains that subsequently coalesce to form the final collapsed state.

Note that in the absence of a torsional potential, we again obtained a hexagonally packed lamellar crystallite but with a shorter fold length. The lamellar structure is still evident and in fact more regular with the increase in adjacently reentrant folds. This, we feel, is a consequence of first forming several small folded domains, which by virtue of their size have a very high incidence of adjacent reentry, and then combining these together to form a single ordered final phase. This feature resembles the regime iii crystallization process in the melt, discussed by Hoffman[16] on the basis of the Gambler's ruin treatment of Guttman et al.[32,33] The latter demands that the probability of tight or regular folds is $\sim^2/_3$. This process requires sets of small clusters, the adjacent stems in each cluster being connected to each other by nonadjacent reentry events. The nonadjacent reentry then arises from the final folding step. Due to the number of short chain segments between the folds, the length of the chain segment between the folds varies over a wide range, from 14 to 30 Å in the current simulation.

The population density of torsion angles along the chain following 720 ps is shown in Figure 4b. It is seen that the trans and near-trans states still predominate. The torsions corresponding to the gauche states are not discrete, but show a broad distribution about the trans conformation, as expected. The torsion energy function is zero only at 180 and ±60°, and the suppression of this term allowed access to a range of conformational states during the dynamics run which could not otherwise be accessed due to the energy barrier. However, when this structure is energy minimized, with the torsional potential, the distribution sharpens, as seen in Figure 5b.

The phenomenon described above has a strong analogy to the isotropic to nematic phase transition in a liquid crystal. In the present case the partially collapsed state displays small domains that are not oriented relative to one another. As the collapse continues, the nonbonded interactions between these microdomains lead to a single orientation direction. In the present simulation we do not have an equilibrium partially collapsed state, but do not rule out the possibility this will occur at higher temperatures. Recent NMR studies of Bremner and Rudin[34] showed that a substantial amount of ordered phase exists in polyethylene melts even after equilibration for long times. From neutron scattering results and electron microscopic studies of ultrahigh molecular weight polyethylene, Schelten et al.[35] and Aharoni et al.[36] concluded that the radius of gyration of the molecules was the same in the melt state as in the bulk. It was also found that crystallization occurs initially within individual molecules and involves one or more of the individual intramolecular domains. The fact that, in spite of the broadening of the distribution of rotational states (Figures 4 and 5), the all-trans conformation still predominates, is in accord with this observation. de Pablo, Laso, and Suter[24] note that with chains of 60 units, at 200 °C, methylene sequences of six trans conformations could still be distinguished in the distribution.

The simulations discussed thus far illustrate that the chain folding of polyethylene into lamellae is a consequence of the long range nonbonded attractive interactions between segments rather than any of the other interactions between the atoms. The addition of a torsional potential term has three important consequences: a longer lamellar length, a strictly global collapse mechanism, and more disorder in the crystallite as measured by the incidence

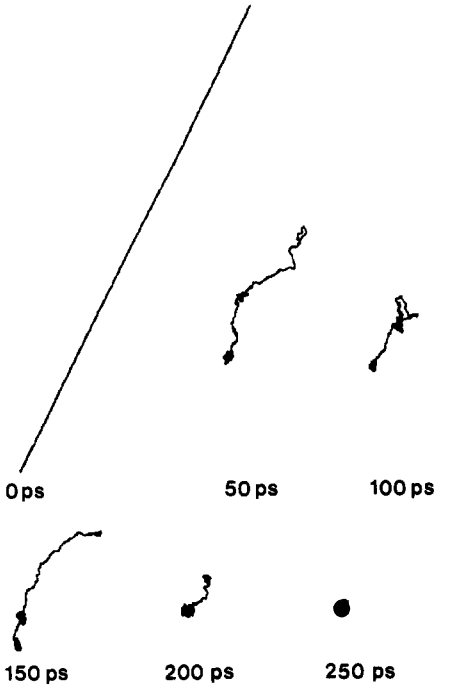

Figure 12. Time evolution of change in shape of a polyethylene chain with 1000 CH_2 units, corresponding to the simulation at 600 K.

of nonadjacent chain folding and reentry. The presence of the torsional potential may simply provide a kinetic barrier to the chain folding process. This could give rise to both the absence of any local collapse phenomena and the longer lamellar fold lengths on average.

Simulations at 600 K. At higher temperatures it is expected that the torsional potential will be less important and a situation similar to the simulations without a torsional potential will arise. This was indeed confirmed in the simulations depicted in Figure 12. In these simulations, which were performed using a temperature of 600 K, we see the collapse of polyethylene occurring through a local followed by global collapse mechanism. After 1000 ps, the average lamellar fold length varies from 23 to 42 Å, which is similar to the case of the "no torsion" simulation. The population density of torsion angles corresponding to the chain after 1000 ps is shown in Figure 4a. The widening of the distribution is clearly seen, although it is not as broad as in Figure 4b without the torsional potential. There is an increase in the population of the gauche states compared to that at 300 K, and the torsion angles corresponding to them are still significantly shifted from ±60°. Upon energy minimizing this structure, the distribution of the torsion angles becomes sharper, with a significant increase in the trans population (Figure 5a). The distribution of states shown in Figures 4 and 5 and the lamellar formation discussed above cast less emphasis on the role of the gauche conformations in the folding process.

Conclusions

The MD simulations reported here have given us some interesting insights into the crystallization processes that may occur in polyethylene, especially when crystallized from very dilute solution. The intersegmental interaction, which dictates the collapse process, stresses the role of the long range attractive forces in the long chain. This work also indicates that the larger R_g measured for melt crystallized polyethylene, as compared to that from solution crystallization, is due to the significant intermolecular interactions which can be expected to be present

in the dense melt. The predominance of near-trans conformation even at higher temperatures is indicative of sustained local order in the polyethylene melt.

Acknowledgment. The authors are grateful to Dr. J. P. Bareman of this laboratory for several useful discussions concerning the molecular dynamics methodology and to the reviewers of this paper for several helpful suggestions.

References and Notes

(1) Keller, A. *Philos. Mag.* **1957**, *2*, 1171.
(2) Mandelkern, L. *Crystallization of Polymers*; McGraw Hill: New York, 1964.
(3) Mandelkern, L. *J. Polym. Sci., Polym. Symp.* **1975**, *50*, 457.
(4) Wunderlich, B. *Macromolecular Physics*; Academic Press: New York, 1973; Vol. 1.
(5) Armitstead, K.; Goldbeck-Wood, G. *Adv. Polym. Sci.* **1992**, *100*, 219.
(6) Privalko, V. P.; Lipatov, Y. S. *Makromol. Chem.* **1974**, *175*, 641.
(7) Corradini, P.; Guerra, G. *Adv. Polym. Sci.* **1992**, *100*, 183.
(8) Sadler, D. M.; Keller, A. *Polymer* **1976**, *17*, 37.
(9) Spells, S. J.; Sadler, D. M. *Polymer* **1984**, *25*, 739.
(10) Flory, P. J. *J. Am. Chem. Soc.* **1962**, *84*, 2857.
(11) Flory, P. J.; Yoon, D. Y. *Nature (London)* **1978**, *272*, 226.
(12) Yoon, D. Y.; Flory, P. J. *Polymer* **1977**, *18*, 509.
(13) Flory, P. J.; Yoon, D. Y. *Discuss. Faraday Soc.* **1979**, *68*, 288.
(14) Sadler, D. M.; Harris, R. *J. Polym. Sci., Polym. Phys. Ed.* **1982**, *20*, 561.
(15) Mansfield, M. L. *Macromolecules 1983*, *16*, 914.
(16) Hoffman, J. D. *Polymer* **1983**, *24*, 3.
(17) Rigby, D.; Roe, R. J. *J. Chem. Phys.* **1987**, *87*, 7285.
(18) Rigby, D.; Roe, R. J. *J. Chem. Phys.* **1988**, *89*, 5280.
(19) Rigby, D.; Roe, R. J. *Macromolecules* **1989**, *22*, 2259.
(20) Rigby, D.; Roe, R. J. In *Computer Simulation of Polymers*; Roe, R. J., Ed.; Prentice Hall: Englewood Cliffs, NJ, 1991; p 79.
(21) Takeuchi, H.; Roe, R. J. *J. Chem. Phys.* **1991**, *94*, 7446.
(22) Takeuchi, H.; Roe, R. J. *J. Chem. Phys.* **1991**, *94*, 7458.
(23) Zúñiga, I.; Bahar, I.; Dodge, R.; Mattice, W. L. *J. Chem. Phys.* **1991**, *95*, 5348.
(24) de Pablo, J. J.; Laso, M.; Suter, U. W. *J. Chem. Phys.* **1992**, *96*, 2395.
(25) Noid, D. W.; Pfeffer, G. A.; Cheng, S. Z. D.; Wunderlich, B. *Macromolecules* **1988**, *21*, 3482.
(26) Sumpter, B. G.; Noid, D. W.; Wunderlich, B.; Cheng, S. Z. D. *Macromolecules* **1990**, *23*, 4671.
(27) Hoover, W. H. *Phys. Rev. A.* **1985**, *31*, 1695.
(28) Mayo, S. L.; Olafson, B. D.; Goddard, W. A., III. *J. Phys. Chem.* **1990**, *94*, 8897.
(29) Sadler, D. M.; Keller, A. *Macromolecules* **1977**, *10*, 1128.
(30) Sadler, D. M.; Keller, A. *Science* **1979**, *203*, 263.
(31) Flory, P. J. *Statistical Mechanics of Chain Molecules*; John Wiley: New York, 1969; p 45.
(32) Gutmann, C. M.; DiMarzio, E. A.; Hoffman, J. D. *Polymer* **1981**, *22*, 1466.
(33) Gutmann, C. M.; DiMarzio, E. A. *Macromolecules* **1982**, *15*, 525.
(34) Bremner, T.; Rudin, A. *J. Polym. Sci., Polym. Phys. Ed.* **1992**, *30*, 1247.
(35) Schelten, J.; Wignall, G. D.; Ballard, D. G. H. *Polymer* **1974**, *15*, 682.
(36) Aharoni, S. M.; Kramer, V.; Vernick, D. A. *Macromolecules* **1979**, *12*, 265.